Journal of Molecular Spectroscopy **204,** 94–105 (2000)
doi:10.1006/jmsp.2000.8192, available online at http://www.idealibrary.com on IDEAL®

The Absorption Spectrum of HDO in the 16 300–16 670 and 18 000–18 350 cm^{-1} Spectral Regions

Alain Campargue, Elena Bertseva, and Olga Naumenko[1]

Laboratoire de Spectrométrie Physique (associated with CNRS UMR C5588), Université Joseph Fourier de Grenoble,
B.P. 87, 38402 Saint-Martin-d'Hères Cedex, France

E-mail: Alain.Campargue@ujf-grenoble.fr

Received May 10, 2000

The absorption spectrum of HDO has been recorded by Intracavity Laser Absorption Spectroscopy in the 16 300–16 670 and 18 000–18 350 cm^{-1} spectral regions corresponding to the weak $2\nu_2 + 4\nu_3$ and $\nu_2 + 5\nu_3$ bands, respectively. The $\nu_2 + 5\nu_3$ band centered at 18 208.434 cm^{-1} was found almost isolated and has been satisfactorily reproduced in the frame of the effective Hamiltonian model. On the other hand, the $2\nu_2 + 4\nu_3$ band at 16 456.201 cm^{-1} is strongly perturbed as the (0 2 4) bright state is involved in a complex interaction scheme including the (1 0 4), (5 0 1), (1 5 2), and (1 11 0) states. The rovibrational assignment of these interacting states was greatly helped by the high-accuracy *ab initio* predictions performed by D. Schwenke and H. Partridge [*J. Chem. Phys.* 000–000 (2000)]. They could be partly modeled by an effective Hamiltonian which has allowed the assignment and reproduction of most of the observed transitions. © 2000 Academic Press

INTRODUCTION

The present study completes our previous investigations of the HDO absorption spectrum in the near-infrared and visible spectral range (*1–4*), by the analysis of two spectral regions, 16 300–16 670 and 18 000–18 350 cm^{-1}, corresponding to the weak $2\nu_2 + 4\nu_3$, $\nu_1 + 4\nu_3$, and the $\nu_2 + 5\nu_3$ absorption bands, respectively, in the vicinity of the much more intense $5\nu_3$ band centered at 16 920.02 cm^{-1} (*4*). Effective Hamiltonian approach together with the recent high-accuracy *ab initio* calculations by Schwenke and Partridge (*5*) were used in the theoretical treatment of the spectra. Both positions and intensities of the HDO absorption lines were considered in the analysis. All the investigated vibrational states were found to be more or less perturbed by the nearby states, yielding considerable intensity transfer in some cases.

In contrast with H_2O, no definite resonance polyad structure has been evidenced in HDO, even for low-lying vibrational states. Resonance interactions do not show regular behavior since in addition to the strong and well-traced Fermi-type interaction (*6–10*), high-order anharmonic and rovibrational couplings between states with large difference of bending quantum numbers have been observed (*2, 3, 9*). These latter interactions seem to be even stronger in HDO compared to H_2O molecule and its symmetric isotope species (*11*) since the ω_1 (2824 cm^{-1}) harmonic frequency of HDO is nearly equal to $2\omega_2$ (2888 cm^{-1}), while in H_2O, these values differ by about 550 cm^{-1}.

The analysis of the HDO absorption spectrum has also proved that high-order anharmonic couplings are rather sensitive to the excitation of the bending mode. For instance, the sequences of the (V_1 0 0) and (0 0 V_3) stretching levels have been found to be well-isolated (*1, 4*), though in some cases, highly excited bending states could be found in the vicinity of them. In contrast, combination states involving one bending excitation such as (V_1 1 0) and (0 1 V_3) appear to be more subject to interactions: the (2 0 0) vibrational state, for example, is slightly perturbed by the other nearby states (*10*), while the $K_a \leq 2$ levels of the (2 1 0) state are half-mixed with those of the (0 5 0) state (*9*). Another case concerns the (0 0 4) state which can be considered as isolated at least up to $J = 9$ (*1*), while the (0 1 4) state is dramatically perturbed through a complex interaction scheme involving the two highly excited bending states, (1 4 2) and (0 12 0) (*2*). In the present paper, we will report the analysis of the rotational structure of the (0 1 5) state which corresponds to one additional bending excitation compared to the well-isolated (0 0 5) state (*4*). In fact, our analysis will show that the (0 1 5) state is only slightly perturbed by the nearby (0 6 3) and (2 7 1) vibrational states in contrast with the situation found for the (0 1 4) state.

The study of the highly excited HDO states above 13 200 cm^{-1} (*1–4*) together with data presented in this paper show that accidental resonances more than a general polyad structure seem to rule the HDO absorption spectrum in the near-infrared and visible ranges. In this context, the high accurate calculations of the HDO absorption spectrum performed by Schwenke and Partridge (*5*) have proven to be highly valuable to identify these casual interactions. The present analysis of the 16 300–

---

[1] On leave from the Institute of Atmospheric Optics, Russian Academy of Sciences, Tomsk, 634055, Russia.

0022-2852/00 $35.00

16 670 cm^{-1} spectral region, corresponding to the $2\nu_2 + 4\nu_3$ and $\nu_1 + 4\nu_3$ perturbed bands, will give more opportunity to prove the importance and the quality of these predictions.

EXPERIMENTAL

Intracavity laser absorption spectroscopy (ICLAS) is an experimental method particularly well suited to explore large spectral regions with a routine sensitivity better than 10^{-8} cm^{-1} (*12*). The cell filled with a 1:1 mixture of H_2O:D_2O was inserted in the laser cavity. In the present experiments, we used our standard standing-wave dye laser (*12*, *13*). Dye solutions of Rhodamine 590 and Rhodamine 560 were used to record the spectra in the 16 300–16 670 and 18 000–18 350 cm^{-1} regions, respectively. The data acquisition system and the procedure used for wavenumber calibration have been previously described (*1*–*4*). The spectral calibration uses as reference absorption lines provided by an iodine cell inserted between the laser and the spectrograph (*14*). We estimate the measured wavenumbers to be precise to within 0.01 cm^{-1} as confirmed by the ground state combination differences provided by the following rotational analysis and by the agreement observed for the H_2O lines with the values given in Refs. (*15*) and (*16*). The relative intensities of the lines were roughly estimated from the peak depth of each line. Despite its limited accuracy, this information will prove to be highly valuable in the spectral assignment process.

RESULTS AND DISCUSSION

A. The $2\nu_2 + 4\nu_3$ and $\nu_1 + 4\nu_3$ Bands

One hundred ninety-nine lines observed in the 16 300–16 670 cm^{-1} spectral region were assigned to HDO and are listed in Table 1. They belong mainly to the $2\nu_2 + 4\nu_3$ and $\nu_1 + 4\nu_3$ bands centered at 16 456.201 and 16 539.04 cm^{-1}, respectively. The rovibrational assignment was performed on the basis of the predictions performed by Schwenke and Partridge (*5*), which are particularly accurate (average deviation of -0.06 cm^{-1}) in this specific region. A comparison of the stick spectrum retrieved from the experiment with the predicted spectrum of Ref. (*5*) is shown in Fig. 1. The weakness of the spectrum under study, with the strongest lines not exceeding 2.8×10^{-6} cm^{-2}/atm, hindered unambiguous assignment of the weakest lines not included into combination differences. Finally, 135 observed lines were attributed to the stronger $2\nu_2 + 4\nu_3$ band, while 42 lines were assigned to the weaker $\nu_1 + 4\nu_3$ band. Nine more transitions borrowing their intensities through resonance intensity transfer could be assigned to the (5 0 1) and (1 11 0) states (vibrational labeling of Ref. (*5*)). Thirteen weak lines (7%) remain unassigned.

Similarly to our previous studies, the experimental relative intensities were normalized to the absolute intensity predicted in Ref. (*5*) by considering the sum of the intensities of the assigned lines. As a result of this normalization procedure, 71% of the measured line intensities could be compared within 20% with their predicted values. The total experimental intensity of the $2\nu_2 + 4\nu_3$ band was calculated to be 1.07×10^{-4} cm^{-2}/atm in close agreement with its predicted (*5*) value of 1.18×10^{-4} cm^{-2}/atm, while the total measured absorption for the $\nu_1 + 4\nu_3$ band (1.27×10^{-5} cm^{-2}/atm) is considerably less than predicted (3.35×10^{-5} cm^{-2}/atm), indicating that many transitions of this weak band were not detected. The $2\nu_2 + 4\nu_3$ band has exclusively *a*-type character, while the $\nu_1 + 4\nu_3$ band has a hybrid character with a predicted *a*:*b* intensity ratio of 1:1.7. The observed line centers, experimental and predicted (*5*) intensities, and rovibrational assignments are included in Table 1. The 104 experimental energy levels obtained from the observed transitions by adding the corresponding experimental levels of the ground state (*17*) appear in Table 2, with the experimental uncertainty and the deviation from their predicted (*5*) values.

Energy considerations indicate that the (0 2 4) vibrational state under study ($E_\nu = 16\,456$ cm^{-1}) may strongly interact with three other nearby states: (1 0 4) at 16 539 cm^{-1}, (5 0 1) at 16 482 cm^{-1}, and (1 5 2) at 16 450 cm^{-1}. According to Ref. (*5*), one more state, (1 11 0), predicted more than 400 cm^{-1} below the above states ($E_\nu = 16\,049$ cm^{-1}), may also perturb the (0 2 4) state since many lines involving its rotational sublevels are predicted with noticeable intensity in the analyzed spectral region. To confirm and extend our rovibrational assignments, we tried to fit the observed energy levels of the five above states, in the frame of the effective Hamiltonian (EH) model in the Padé–Borel representation (*18, 19*). It appeared to be rather easy to account for the (0 2 4)–(1 0 4)–(5 0 1) interactions: the rotational levels of the (0 2 4) and (1 0 4) states with $K_a \geq 3$ strongly interact via Fermi resonance, while a high-order anharmonic interaction strongly connects some of the $K_a = 1$, 2 levels of the (0 2 4) and (5 0 1) states. Sixty-eight of the 104 observed levels, including two energy levels of the (5 0 1) dark state, could be fitted using this interaction scheme with an rms deviation of 0.030 cm^{-1}. The fitted values of the rovibrational parameters obtained for the (0 2 4), (1 0 4), and (5 0 1) states are presented in Table 3. One important result of the fitting is that the center of the $\nu_1 + 4\nu_3$ band could be retrieved at 16 539.042(16) cm^{-1} despite the fact that the energy of the (1 0 4) [000] level could not be experimentally determined. Note that all the $K_a = 0$, 1 energy levels of the (0 2 4) state were excluded from the fit (see Table 2). They are indeed affected by an extra interaction (see below) which makes them deviate significantly (up to 1.6 cm^{-1}) from their EH predicted values. The mixing coefficients calculated in the EH approach for the high K_a levels indicate that the vibrational assignment given in Ref. (*5*) for some of these levels should be interchanged between the (1 0 4) and (0 2 4) states. This reassignment is confirmed by the fact that the stronger lines correspond now to the $2\nu_2 + 4\nu_3$ band, while weaker lines belong to the $\nu_1 + 4\nu_3$ band.

TABLE 1
Wavenumbers, Intensities, and Rovibrational Assignments of the HDO Absorption Lines between 16 300 and 16 670 cm^{-1}

Observed Wavenumber (cm^{-1})	Intensity (cm^{-2}/atm)		Upper $J K_a K_c$	Lower $J K_a K_c$	Vib. state
	Obs.	Ref. (5)			
16304.373	4.0E-07	2.0E-07	8 2 7	9 2 8	0 2 4
16305.053	2.9E-07	2.3E-07	8 1 8	9 1 9	0 2 4
16306.060	2.2E-07	2.1E-07	8 1 7	9 1 8	0 2 4
16306.448	3.3E-07	3.4E-07	8 0 8	9 0 9	0 2 4
16306.718	2.7E-07	1.2E-07	7 4 4	8 4 5	0 2 4
16306.718	2.7E-07	1.2E-07	7 4 3	8 4 4	0 2 4
16316.734	4.9E-07	2.0E-07	7 3 5	8 3 6	0 2 4
16317.028	2.8E-07	2.3E-07	7 3 4	8 3 5	0 2 4
16321.487	3.9E-07	3.0E-07	7 2 5	8 2 6	0 2 4
16322.398	4.4E-07	3.3E-07	7 2 6	8 2 7	0 2 4
16323.744	4.0E-07	1.8E-07	6 4 3	7 4 4	0 2 4
16323.744	4.0E-07	1.8E-07	6 4 2	7 4 3	0 2 4
16323.994	3.5E-07	3.8E-07	7 1 6	8 1 7	0 2 4
16325.956	7.2E-07	5.7E-07	7 0 7	8 0 8	0 2 4
16325.956	7.2E-07	5.1E-07	7 1 7	8 1 8	0 2 4
16333.389	3.5E-07	3.5E-07	6 3 3	7 3 4	0 2 4
16333.614	5.0E-07	2.7E-07	6 3 4	7 3 5	0 2 4
T 16333.614	5.0E-07	9.8E-08	3 3 1	4 4 0	1 0 4
16337.605	5.7E-07	4.7E-07	6 2 4	7 2 5	0 2 4
16338.464	3.2E-07	2.3E-07	6 2 5	7 2 6	5 0 1
16340.196	3.9E-07	3.2E-07	6 2 5	7 2 6	0 2 4
16340.613	4.5E-07	2.2E-07	5 4 2	6 4 3	0 2 4
16340.613	4.5E-07	2.2E-07	5 4 1	6 4 2	0 2 4
16341.042	6.6E-07	6.2E-07	6 1 5	7 1 6	0 2 4
16344.230	8.0E-07	7.9E-07	6 1 6	7 1 7	0 2 4
16344.524	7.5E-07	8.1E-07	6 0 6	7 0 7	0 2 4
16349.926	5.5E-07	5.0E-07	5 3 2	6 3 3	0 2 4
16350.035	4.4E-07	3.8E-07	5 3 3	6 3 4	0 2 4
16354.245	4.3E-07	5.5E-07	5 2 3	6 2 4	0 2 4
16356.309	5.9E-07	7.7E-07	5 2 4	6 2 5	0 2 4
16357.264	1.2E-06	9.3E-07	5 1 4	6 1 5	0 2 4
16357.264	1.2E-06	1.8E-07	4 4 1	5 4 2	0 2 4
16357.264	1.2E-06	1.8E-07	4 4 0	5 4 1	0 2 4
16361.626	1.1E-06	9.8E-07	5 1 5	6 1 6	0 2 4
16362.128	1.1E-06	1.1E-06	5 0 5	6 0 6	0 2 4
16366.371	3.5E-07	3.1E-07	4 3 2	5 3 3	0 2 4
16366.591	5.7E-07	5.8E-07	4 3 1	5 3 2	0 2 4
16368.972	3.1E-07	3.0E-07	4 2 2	5 3 3	1 0 4
16369.904	1.0E-06	9.2E-07	4 2 2	5 2 3	0 2 4
16372.725	1.1E-06	9.5E-07	4 2 3	5 2 4	0 2 4
16372.936	1.2E-06	1.2E-06	4 1 3	5 1 4	0 2 4
16376.638	3.5E-07	2.4e-07	4 1 4	5 1 5	1 11 0
16378.643	1.3E-06	1.3E-06	4 0 4	5 0 5	0 2 4
16379.718	1.1E-06	1.1E-06	4 1 4	5 1 5	0 2 4
16380.560	2.2E-07	1.7E-07	4 1 4	5 0 5	1 11 0
16383.108	4.9E-07	5.0E-07	3 3 0	4 3 1	0 2 4
16383.780	4.9E-07	4.6E-07	3 2 1	4 3 2	1 0 4
16386.790	9.7E-07	9.9E-07	3 2 1	4 2 2	0 2 4
16388.839	9.7E-07	9.9E-07	3 2 2	4 2 3	0 2 4
16389.029	1.3E-07	3.9E-08	3 0 3	3 2 2	0 2 4
16389.246	1.3E-06	1.4E-06	3 1 2	4 1 3	0 2 4
16394.269	1.3E-06	1.2E-06	3 0 3	4 0 4	0 2 4
16395.508	1.5E-06	1.5E-06	3 1 3	4 1 4	0 2 4
16395.657	3.5E-07	4.2E-07	3 1 3	4 0 4	1 11 0
16398.465	1.8E-07	1.5E-07	2 2 1	3 3 0	1 0 4
16399.007	1.4E-07	1.5E-07	2 2 0	3 3 1	1 0 4
16400.669	1.6E-07				
16403.642	7.8E-07	7.5E-07	2 2 0	3 2 1	0 2 4
16404.745	7.9E-07	7.4E-07	2 2 1	3 2 2	0 2 4
16405.196	1.4E-06	1.4E-06	2 1 1	3 1 2	0 2 4
16406.552	2.3E-07	9.7E-08	5 1 4	6 2 5	1 0 4
16409.408	1.8E-07	9.0E-08	3 1 3	4 2 2	1 0 4
16409.743	1.4E-06	1.4E-06	2 0 2	3 0 3	0 2 4
16411.061	1.6E-06	1.4E-06	2 1 2	3 1 3	0 2 4
16411.468	3.5E-07	1.1E-07	7 5 3	7 5 2	0 2 4
16411.468	3.5E-07	1.1E-07	7 5 2	7 5 3	0 2 4
16413.472	1.8E-07				
16413.830	3.5E-07	2.1E-07	6 5 1	6 5 2	0 2 4
16413.830	3.5E-07	2.2E-07	6 5 2	6 5 1	0 2 4
16415.843	8.4E-07	4.2E-07	5 5 1	5 5 0	0 2 4
16415.843	8.4E-07	4.2E-07	5 5 0	5 5 1	0 2 4
16421.506	1.1E-06	9.9E-07	1 1 0	2 1 1	0 2 4
16421.835	1.5E-07	1.5E-07	6 0 6	7 1 7	1 0 4
16425.188	1.3E-06	1.3E-06	1 0 1	2 0 2	0 2 4
16426.146	1.0E-06	1.0E-06	1 1 1	2 1 2	0 2 4
16428.112	2.2E-07	8.4E-08	6 6 1	6 6 0	0 2 4
16428.112	2.2E-07	8.4E-08	6 6 0	6 6 1	0 2 4
16431.652	2.9E-07	1.4E-07	7 4 4	7 4 3	0 2 4
16431.652	2.9E-07	1.4E-07	3 1 2	4 2 3	1 0 4
16432.760	1.9E-07	1.4E-07	7 4 3	7 4 4	0 2 4
16433.087	2.8E-07	3.1E-07	6 4 3	6 4 2	0 2 4
16433.404	3.3E-07	3.1E-07	6 4 2	6 4 3	0 2 4
16434.265	6.7E-07	5.8E-07	5 4 2	5 4 1	0 2 4
16434.314	6.7E-07	5.8E-07	5 4 1	5 4 2	0 2 4
16434.706	1.9E-07	1.1E-07	5 2 4	5 3 3	1 0 4
16435.197	2.1E-06	1.0E-06	4 4 1	4 4 0	0 2 4
16435.197	2.1E-06	1.0E-06	4 4 0	4 4 1	0 2 4
16435.429	3.4E-07	3.1E-07	3 1 3	3 1 2	0 2 4
16436.388	1.9E-07	1.5E-07	7 3 5	7 3 4	0 2 4
16437.209	3.2E-07	3.0E-07	5 2 4	5 2 3	0 2 4
16439.141	1.8E-07	2.0E-07	5 0 5	6 1 6	1 0 4
16440.693	7.1E-07	7.7E-07	0 0 0	1 0 1	0 2 4
16440.850	2.7E-07	2.8E-07	6 3 4	6 3 3	0 2 4
16443.013	4.4E-07	2.8E-07	3 2 2	3 3 1	1 0 4
16443.013	4.4E-07	1.9E-07	5 1 5	6 0 6	1 0 4
16443.156	5.6E-07	5.8E-07	5 3 3	5 3 2	0 2 4
16444.367	8.5E-07	1.0E-06	4 3 2	4 3 1	0 2 4
16444.534	4.9E-07	5.7E-07	4 2 3	4 2 2	0 2 4
16444.968	1.2E-06	1.3E-06	3 3 1	3 3 0	0 2 4
16445.262	6.2E-07	5.5E-07	2 1 2	2 1 1	0 2 4
16445.522	8.1E-07	8.4E-07	4 3 1	4 3 2	0 2 4
16445.752	1.4E-06	1.4E-06	3 3 0	3 3 1	0 2 4
16445.918	5.0E-07	4.8E-07	5 3 2	5 3 3	0 2 4
16446.204	4.9E-07	4.3E-07	3 2 1	3 3 0	1 0 4
16447.844	3.6E-07	2.4E-07	6 3 3	6 3 4	0 2 4
16448.810	1.1E-06	1.0E-06	3 2 2	3 2 1	0 2 4
16449.125	1.8E-07	4.3E-08	6 5 2	6 5 1	1 0 4
16449.125	1.8E-07	4.3E-08	6 5 1	6 5 2	1 0 4
16450.864	1.8E-06	1.9E-06	2 2 1	2 2 0	0 2 4
16451.780	2.8E-06	1.2E-06	1 1 1	1 1 0	0 2 4
16451.780	2.8E-06	1.8E-06	2 2 0	2 2 1	0 2 4
16453.226	1.0E-06	1.0E-06	3 2 1	3 2 2	0 2 4
16455.090	4.0E-07	1.4E-07	1 1 1	2 2 0	1 0 4
16455.090	4.0E-07	2.2E-07	4 0 4	5 1 5	1 0 4

Note. The experimental and predicted (*5*) intensities are given in cm^{-2}/atm at 296 K and correspond to pure HDO. The total experimental absorption of HDO is normalized to that predicted in Ref. (*5*) (see text). T means tentative assignment. Lines blended by $H_2{}^{16}O$ lines are marked (*b*). In the case of unresolved multiplets, the same experimental intensity is given for the different components, while the intensities from Ref. (*5*) correspond to each component. Some lines in the high-frequency edge of the observed spectrum belonging to the $5\nu_3$ band were excluded from the list.

TABLE 1—*Continued*

Observed Wavenumber (cm^{-1})	Intensity (cm^{-2}/atm)		Upper $J\,K_a\,K_c$	Lower $J\,K_a\,K_c$	Vib. State
	Obs.	Ref. (*5*)			
16455.665	1.8E-07	1.0E-07	5 1 5	5 2 4	1 0 4
16456.860	5.6E-07	5.5E-07	4 2 2	4 2 3	0 2 4
16457.879	1.1E-06	1.2E-06	1 1 0	1 1 1	0 2 4
16458.391	1.9E-07	1.6E-07	1 1 0	2 2 1	1 0 4
16459.002	1.8E-07	5.0E-08	3 2 2	4 2 3	1 0 4
16459.002	1.8E-07	1.1E-07	4 0 4	5 0 5	1 0 4
16462.104	1.8E-07	1.9E-07	4 1 4	5 0 5	1 0 4
16463.534	6.2E-07	5.5E-07	2 1 1	2 1 2	0 2 4
16464.152	1.8E-07	1.7E-07	5 2 3	5 2 4	0 2 4
16465.705	1.8E-07	9.2E-08	3 1 2	4 1 3	1 0 4
16469.479	2.7E-07	2.4E-07	3 0 3	4 1 4	1 0 4
16471.358	8.0E-07	8.3E-07	1 0 1	0 0 0	0 2 4
16471.832	2.7E-07	3.0E-07	3 1 2	3 1 3	0 2 4
16481.636	9.7E-07	1.1E-06	2 1 2	1 1 1	0 2 4
16482.810	3.1E-07	2.3E-07	2 0 2	3 1 3	1 0 4
16483.599	2.1E-07	9.7E-08	2 1 1	3 1 2	1 0 4
16485.564	1.3E-06	1.4E-06	2 0 2	1 0 1	0 2 4
16489.165	1.1E-06	1.1E-06	2 1 1	1 1 0	0 2 4
16490.913	2.3E-07	1.6E-07	4 1 3	4 2 2	1 0 4
16491.628	2.4E-07	1.5E-07	3 1 2	3 2 1	1 0 4
16493.765	1.4E-06	1.7E-06	3 1 3	2 1 2	0 2 4
16496.948	9.7E-07	9.0E-07	3 2 2	2 2 1	0 2 4
16498.262	1.5E-06	1.5E-06	3 0 3	2 0 2	0 2 4
16499.357	9.9E-07	8.9E-07	3 2 1	2 2 0	0 2 4
16499.643	5.6E-07	4.6E-07	3 1 3	2 0 2	1 11 0
16502.111	4.3E-07	3.7E-07	4 1 4	3 1 3	1 11 0
16505.207	1.3E-06	1.5E-06	4 1 4	3 1 3	0 2 4
16506.055	1.3E-06	1.6E-06	3 1 2	2 1 1	0 2 4
16507.030	8.0E-07	5.0E-07	4 3 2	3 3 1	0 2 4
16507.030	8.0E-07	7.5E-08	6 5 1	5 5 0	0 2 4
16507.030	8.0E-07	7.5E-08	6 5 2	5 5 1	0 2 4
16507.964	5.9E-07	5.0E-07	4 3 1	3 3 0	0 2 4
16509.275	1.7E-06	1.9E-06	4 0 4	3 0 3	0 2 4
16510.980	1.2E-06	1.3E-06	4 2 3	3 2 2	0 2 4
16511.169	2.7E-07	1.8E-07	4 1 4	3 0 3	1 11 0
16512.226	3.5E-07	2.4E-07	5 4 2	4 4 1	0 2 4
16512.226	3.5E-07	2.4E-07	5 4 1	4 4 0	0 2 4
16513.850	1.4E-06	1.7E-06	5 1 5	4 1 4	0 2 4
16516.833	1.1E-06	1.2E-06	4 2 2	3 2 1	0 2 4
16516.998	3.5E-07	2.5E-07	2 0 2	2 1 1	1 0 4
16518.277	1.8E-06	1.9E-06	5 0 5	4 0 4	0 2 4
16521.714	1.3E-06	1.7E-06	4 1 3	3 1 2	0 2 4
16522.071	7.6E-07	7.1E-07	5 3 3	4 3 2	0 2 4
16522.808	1.5E-06	1.6E-06	6 1 6	5 1 5	0 2 4
16523.914	6.2E-07	6.7E-07	5 3 2	4 3 1	0 2 4
16524.148	1.2E-06	1.3E-06	5 2 4	4 2 3	0 2 4
16525.742	1.4E-06	1.6E-06	6 0 6	5 0 5	0 2 4
16526.834	3.2E-07	3.0E-07	6 4 3	5 4 2	0 2 4
16527.044	4.2E-07	3.0E-07	6 4 2	5 4 1	0 2 4
16529.401	2.6E-07				
16530.573	1.3E-06	1.2E-06	7 1 7	6 1 6	0 2 4
16531.695	3.2E-07				
16531.850	1.8E-07	8.8E-08	1 1 1	1 1 0	1 0 4
16532.129	1.3E-06	1.3E-06	7 0 7	6 0 6	0 2 4
16533.784	1.9E-07	1.8E-07	5 2 3	4 2 2	5 0 1
b 16535.266	8.8E-07	4.0E-07	6 2 5	5 2 4	5 0 1
16535.436	4.4E-07	5.0E-07	8 1 8	7 1 7	0 2 4
16535.974	8.6E-07	8.7E-07	5 2 3	4 2 2	0 2 4
16536.795	1.9E-06	1.6E-06	5 1 4	4 1 3	0 2 4
16536.795	1.9E-06	6.2E-07	6 3 4	5 3 3	0 2 4
16536.987	7.9E-07	7.0E-07	6 2 5	5 2 4	0 2 4
16537.715	9.7E-07	8.3E-07	8 0 8	7 0 7	0 2 4
16540.943	6.9E-07	6.1E-07	6 3 3	5 3 2	0 2 4
b 16541.386	4.6E-07	2.5E-07	7 4 4	6 4 3	0 2 4
16542.166	6.8E-07	2.5E-07	7 4 3	6 4 2	0 2 4
16542.166	6.8E-07	5.3E-07	9 0 9	8 0 8	0 2 4
16547.444	5.1E-07	7.9E-07	7 2 6	6 2 5	0 2 4
16549.029	2.6E-07				
16549.714	8.8E-07	1.3E-06	6 1 5	5 1 4	0 2 4
16550.823	6.0E-07	5.2E-07	7 3 5	6 3 4	0 2 4
16552.906	2.2E-07				
16553.726	8.2E-07	9.4E-07	6 2 4	5 2 3	0 2 4
16557.041	7.1E-07	5.5E-07	8 2 7	7 2 6	0 2 4
16557.369	2.3E-07	2.6E-07	3 1 2	3 0 3	1 0 4
16557.901	4.0E-07	1.9E-07	5 2 3	5 1 4	1 0 4
16557.901	4.0E-07	1.4E-07	6 2 4	6 1 5	1 0 4
16559.163	5.3E-07	4.8E-07	7 3 4	6 3 3	0 2 4
16559.652	2.1E-07	2.0E-07	4 2 2	4 1 3	1 0 4
16560.062	7.7E-07	8.5E-07	7 1 6	6 1 5	0 2 4
16563.976	5.3E-07	3.6E-07	8 3 6	7 3 5	0 2 4
16565.416	3.5E-07	3.3E-07	9 2 8	8 2 7	0 2 4
16567.714	3.5E-07	1.5E-07	2 0 2	1 0 1	1 0 4
16567.714	3.5E-07	1.7E-07	3 0 3	2 1 2	1 0 4
16567.867	5.3E-07	5.7E-07	8 1 7	7 1 6	0 2 4
16569.490	2.7E-07	1.4E-07	5 1 4	5 0 5	1 0 4
16571.034	6.2E-07	7.2E-07	7 2 5	6 2 4	0 2 4
16571.314	1.3E-07	1.2E-07	10 2 9	9 2 8	0 2 4
16573.931	5.9E-07	3.0E-07	9 1 8	8 1 7	0 2 4
16573.931	5.9E-07	1.1E-07	9 4 5	8 4 4	0 2 4
16575.952	3.7E-07	2.2E-07	9 3 7	8 3 6	0 2 4
16576.897	2.7E-07	1.6E-07	10 1 9	9 1 8	0 2 4
16579.704	2.9E-07	1.9E-07	3 0 3	2 0 2	1 0 4
16582.499	2.7E-07	1.3E-07	3 1 2	2 1 1	1 0 4
16582.499	2.7E-07	7.8E-08	5 2 4	5 1 5	1 0 4
16586.330	4.9E-07	4.4E-07	8 2 6	7 2 5	0 2 4
16591.360	2.7E-07	2.1E-07	5 0 5	4 1 4	1 0 4
16592.717	3.7E-07	2.5E-07	4 1 4	3 0 3	1 0 4
16599.016	2.2E-07	1.7E-07	2 2 1	1 1 0	1 0 4
b 16599.392	3.7E-07	2.8E-07	9 2 7	8 2 6	0 2 4
16600.418	3.5E-07	1.8E-07	6 0 6	5 1 5	1 0 4
16604.328	3.1E-07	1.8E-07	6 0 6	5 0 5	1 0 4
16609.864	2.0E-07	1.4E-07	3 2 2	2 1 1	1 0 4
16632.554	2.3E-07				
16642.255	1.7E-07	7.8E-08	4 2 2	3 1 3	1 0 4
16644.042	3.8E-07				
16645.386	1.6E-07				
16656.583	6.6E-07	1.0E-07	5 3 2	4 2 3	1 0 4
16658.758	2.6E-07	8.0E-08	6 3 4	5 2 3	1 0 4
16665.545	2.8E-07				
16666.050	3.0E-07				
16670.453	2.6E-07				
16671.110	1.4E-07				

At the second step, we tried to fit all the observed energy levels using an interacting scheme involving the five vibrational states. As a result, we found that the $K_a = 0, 1$ energy levels of the (0 2 4) state strongly interact both through anharmonic and rovibrational resonances with the (1 5 2) and (1 11 0) highly excited bending states. This resonance scheme is very similar to that affecting the (0 1 4) state for which the $K_a = 0, 1$ levels were found to be perturbed by the (1 4 2) and

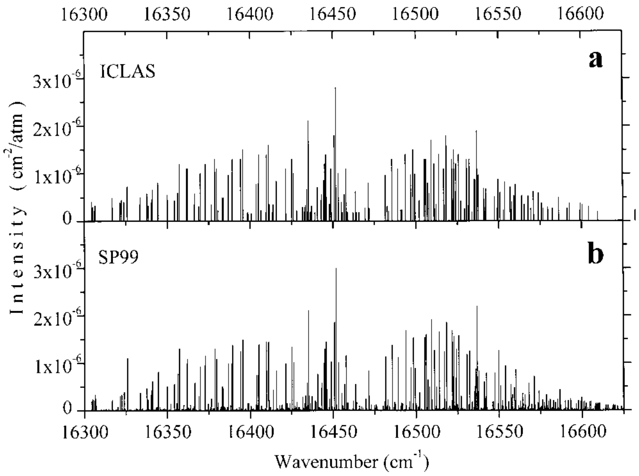

FIG. 1. Comparison of the overview of the HDO absorption spectrum between 16 300 and 16 670 cm^{-1}. (a) Stick spectrum retrieved from the ICLAS spectrum. The absolute intensities were obtained after normalization of the experimental data against the corresponding absorption intensity predicted (*5*) in the analyzed region (see text). (b) Calculated spectrum predicted by the *ab initio* calculations of Ref. (*5*). Some lines in the high-frequency edge of the spectrum belonging to the $5\nu_3$ band were excluded both from the observed spectrum and from the predicted spectrum (*5*).

(0 12 0) states (*2*). The occurrence of such high-order resonance interactions in HDO molecule has been already discussed in Ref. (*2*). Though the perturbations observed for the $K_a = 0$, 1 sublevels of the (0 2 4) are large, we could identify only two additional levels, at 16 545.814 and 16 602.502 cm^{-1}, observed through six additional lines, which borrow their intensity from the corresponding line partners of the $2\nu_2 + 4\nu_3$ band. Considering the limited experimental information relative to the (1 5 2) and (1 11 0) dark states, the difficulty to estimate reasonably the unperturbed rotational constants of these states, our attempts to perform a complete fit of all the observed energy levels were not satisfactory enough to be presented here. However, the EH calculations suggest that the two above additional energy levels, assigned in Ref. (*5*) as (0 2 4) [303] and (0 2 4) [414] levels, respectively, should be, in fact, reassigned to (1 11 0) [313] and (1 11 0) [414], respectively.

Figure 2 shows the excellent agreement between the observed and predicted (*5*) spectra between 16 498 and 16 536 cm^{-1}. Five lines of the $5\nu_1 + \nu_3$ and $\nu_1 + 11\nu_2$ bands borrowing their intensities through resonance transfer are indicated.

B. The $\nu_2 + 5\nu_3$ Band

The $\nu_2 + 5\nu_3$ band centered at 18 208.434 cm^{-1} is the most excited overtone transition of HDO analyzed so far. It is a rather weak band of exclusively *a* type with line intensities not exceeding 2.2×10^{-6} cm^{-2}/atm. Overall, 173 absorption lines were attributed to the HDO species in the 18 000–18 350 cm^{-1} spectral region. Most of the observed transitions belong to the $\nu_2 + 5\nu_3$ band, while seven transitions borrowing their intensities through resonance interaction with the main band involve rotational sublevels of the (1 1 4) state and the (0 6 3) and (2 7 1) highly excited bending states. As in the above analysis, line positions and intensity calculations within the effective Hamiltonian (EH) approach, together with the high-accuracy *ab initio* predictions of Ref. (*5*), were systematically used in the identification process.

The experimental intensities were normalized against the absolute values predicted in Ref. (*5*), as described above. In the determination of the normalizing factor, 64% of the measured line intensities were compared with their predicted (*5*) values yielding an average agreement of 16%. Figure 3 shows the overview of the observed, simulated (EH), and predicted (*5*) spectrum of the $\nu_2 + 5\nu_3$ band. The list of the 173 measured line positions, the corresponding experimental, calculated (see below), and predicted (*5*) intensities followed by the rotational assignment is presented in Table 4. Except for seven weak lines (4%), all the transitions could be rovibrationally assigned.

The experimental energy levels of the (0 1 5) vibrational state are gathered in Table 5. The theoretical treatment of the observed line positions and intensities show that the resonance interactions of the (0 1 5) state with the nearby states are surprisingly weak compared to the (0 1 4) situation. It allows in a good approximation, the (0 1 5) state to be treated as an isolated vibrational state. Finally, 74 of the 80 experimental energy levels could be reproduced within 0.024 cm^{-1} by the EH. This rms deviation is significantly larger than the experimental accuracy on the energy levels (0.004 cm^{-1} for the levels obtained from combination differences of two or more lines). The deviations of the observed energy levels from their calculated (EH) and predicted (*5*) values are also given in Table 5 for comparison. It is interesting to note that Ref. (*5*) predicts the energy levels of the (0 1 5) state with a nearly constant shift of 0.7 cm^{-1} up to $J = 8$, while the deviations increase up to 1.8 cm^{-1} for $J = 11$. The fitted values of the rotational and centrifugal distortion parameters are listed in Table 6.

The rovibrational wavefunctions obtained from the energy level fittings were then used to derive two transition moment parameters ($\mu_1 = 2.455(40) \times 10^{-5}$ D and $\mu_2 = 5.48(60) \times 10^{-8}$ D) from the fitting to the normalized experimental intensities of 74 unblended lines. These parameters provide an average accuracy of 11% in the reproduction of the input data. The line intensities calculated with these transition moment parameters are included in Table 4. The total calculated band intensity is 1.47×10^{-4} cm^{-2}/atm in agreement with a predicted (*5*) value of 1.56×10^{-4} cm^{-2}/atm. Figures 3 and 4 show a comparison of the observed, calculated, and predicted (*5*) spectra for the whole and an expanded regions, respectively.

Among the six perturbed energy levels excluded from the fit, five deviate from their unperturbed positions by less than 0.17 cm^{-1}, while the [4 1 4] level is shifted by $+0.38$ cm^{-1}. This last level is the only one for which the assignment of the perturbers

TABLE 2

Rotational Energy Levels (cm^{-1}) of the (0 2 4), (1 0 4), (1 11 0), and (5 0 1) Vibrational States of HDO

	(0 2 4)				(1 0 4)				(1 11 0)				(5 0 1)			
$J\,K_a\,K_c$	E_{obs}	σ	N	Δ	E_{obs}	σ	N	Δ	E_{obs}	σ	N	Δ	E_{obs}	σ	N	Δ
0 0 0	*16456.201		1	0.00												
1 0 1	*16471.359	0.001	2	-0.03												
1 1 1	*16484.274	0.002	2	-0.04	*16564.352	0.006	2	-0.12								
1 1 0	*16487.689	0.001	2	-0.03	16567.316		1	-0.12								
2 0 2	*16501.072	0.001	2	-0.04	16583.201	0.016	3	-0.11								
2 1 2	*16511.447	0.003	3	-0.02												
2 1 1	*16521.659	0.002	3	-0.03	16600.060		1	-0.09								
2 2 1	16560.133	0.001	2	-0.05	16631.514	0.002	2	-0.11								
2 2 0	16560.706	0.001	2	-0.04	16632.030		1	-0.13								
3 0 3	*16544.425	0.007	3	-0.03	16625.868	0.008	2	-0.10								
3 1 3	*16551.891	0.001	3	-0.02	16631.244		1	-0.12	*16545.814	0.002	2	0.04				
3 1 2	*16572.230	0.007	3	-0.01	16648.691	0.005	5	-0.12								
3 2 2	16605.876	0.003	3	-0.04	16676.043	0.005	3	-0.09								
3 2 1	16608.622	0.005	3	-0.04	16679.260	0.006	2	-0.07								
3 3 1	16678.018		1	-0.06												
3 3 0	16678.780	0.005	2	-0.03												
4 0 4	*16600.597	0.008	2	-0.02	16680.954	0.005	3	-0.10								
4 1 4	*16605.590	0.007	2	0.00	16684.048	0.002	2	-0.13	*16602.502	0.003	4	0.02				
4 1 3	*16638.173	0.002	2	-0.06	16712.749		1	-0.13								
4 2 3	16666.366	0.004	3	-0.03												
4 2 2	16673.899	0.002	3	-0.04	16742.639	0.004	3	-0.10								
4 3 2	16740.045	0.007	3	-0.03												
4 3 1	16741.008	0.006	3	-0.03												
4 4 1	16837.517	0.010	2	-0.03												
4 4 0	16837.524	0.001	2	-0.04												
5 0 5	*16668.437	0.005	2	-0.02	*16747.749	0.007	2	-0.11								
5 1 5	*16670.237	0.005	2	-0.04	16749.314	0.013	2	-0.14								
5 1 4	*16719.774	0.003	2	-0.01	16791.431	0.004	2	-0.11								
5 2 4	16741.192	0.008	3	-0.02	16808.367	0.004	2	-0.06								
5 2 3	16757.797	0.009	3	-0.09	16823.137		1	-0.10					16755.620		1	0.06
5 3 3	16817.557	0.007	3	-0.02												
5 3 2	16819.588	0.004	3	-0.02	*16873.624		1	-0.12								
5 4 2	16914.527	0.021	3	-0.02												
5 4 1	16914.570	0.013	2	-0.03												
5 5 1	17031.811		1	-0.03												
5 5 0	17031.811		1	-0.04												
6 0 6	*16747.686	0.001	2	-0.03	*16826.279	0.004	3	-0.09								
6 1 6	*16748.674	0.002	2	-0.05												
6 1 5	16814.954	0.005	2	-0.03												
6 2 5	16830.623	0.001	2	0.04									16828.897	0.006	2	0.18
6 2 4	16857.724	0.004	2	-0.07	16920.408		1	-0.10								
6 3 4	16910.516	0.002	2	-0.02	*16962.752		1	-0.09								
6 3 3	16915.354	0.003	3	0.00												
6 4 3	17007.067	0.008	3	-0.03												
6 4 2	17007.298	0.004	2	-0.04												
6 5 2	17122.998	0.001	2	-0.05	17158.292		1	-0.08								
6 5 1	17122.998	0.001	2	-0.05	17158.291		1	-0.06								
6 6 1	17300.902		1	-0.01												
6 6 0	17300.902		1	-0.03												
7 0 7	*16838.457	0.014	2	-0.04												
7 1 7	*16839.188		1	-0.06												
7 1 6	*16922.563	0.006	2	-0.03												
7 2 6	16932.331	0.013	2	-0.04												
7 2 5	16974.579	0.004	2	-0.05												
7 3 5	17018.347	0.007	3	-0.05												
7 3 4	17028.825	0.002	2	-0.02												
7 4 4	17115.273	0.008	3	-0.04												
7 4 3	17116.123	0.013	2	-0.07												
7 5 3	17229.481		1	-0.08												
7 5 2	17229.474		1	-0.07												
8 0 8	*16940.876	0.001	2	-0.17												
8 1 8	*16939.844		1	-0.07												
8 1 7	*17041.789	0.005	2	-0.04												
8 2 7	17047.469	0.001	2	-0.04												
8 2 6	*17106.453		1	-0.10												
8 3 6	17140.881		1	-0.13												
9 0 9	17054.681		1	-0.21												
9 1 8	*17172.494		1	-0.04												
9 2 8	*17175.363		1	-0.12												
9 2 7	17252.480		1	-0.15												
9 3 7	17277.572		1	-0.18												
9 4 5	17383.324		1	-0.08												
10 1 9	*17312.632		1	-0.14												
10 2 9	*17314.411		1	-0.14												

Note. Asterisks denote the energy levels excluded from the fitting. σ denotes the experimental uncertainty of the level in cm^{-1}. N is the number of lines sharing the same upper level. Δ is the difference between the experimental and predicted (*5*) values of the energy.

TABLE 3
Spectroscopic Constants of the (0 2 4), (1 0 4), and (5 0 1) Vibrational States of HDO (in cm^{-1})

	(0 2 4)	(1 0 4)	(5 0 1)
E_v	16454.9930(370)	16539.0421(160)	16481.89
A	22.66089(770)	19.40705(630)	19.9396(340)
B	9.34937(310)	8.91221(110)	8.38238(670)
C	5.91155(350)	5.97623(120)	5.9
Δ_k	$4.5517(200) \times 10^{-2}$	$8.586(300) \times 10^{-3}$	9.1×10^{-3}
Δ_{jk}	$-1.902(160) \times 10^{-3}$	3.0×10^{-4}	3.0×10^{-4}
Δ_j	$4.656(210) \times 10^{-4}$	4.2×10^{-4}	4.2×10^{-4}
δ_k	$5.238(180) \times 10^{-3}$	1.6×10^{-3}	1.6×10^{-3}
δ_j	$3.258(180) \times 10^{-4}$	1.5×10^{-4}	1.5×10^{-4}
H_k	9.7×10^{-4}	3.3×10^{-5}	3.3×10^{-5}

Coupling Constants

	F_k	F_j	F_{xy}	C_{xz}
(104)-(024)	-0.52724(370)	$-8.381(270) \times 10^{-2}$		
(104)-(024)				-0.5351(100)
(501)-(024)	$-6.16(120) \times 10^{-2}$	$2.802(130) \times 10^{-2}$	$2.283(170) \times 10^{-2}$	

Note. All the energy levels of the (0 2 4) state with $K_a = 0, 1$, greatly perturbed by interaction with the (1 5 2) and (1 11 0) states, were excluded from the fit. Parameters presented without confidence interval were fixed to the correspondent values of the (1 2 0) state (*10*) for the (0 2 4) and the values of the (0 0 4) state (*1*) for the (1 0 4) and (5 0 1) states.

could be supported by the observation of extra lines. According to the predictions of Ref. (*5*), this energy level is perturbed by two states leading to a considerable intensity transfer to several resonance line partners. This intensity transfer seems to be confirmed both by the observation of three resonance line partners and by the overestimation of the EH calculated intensities of the transitions involving the [414] (0 1 5) level (see Fig. 4). The vibrational assignment of the perturbers is difficult, as Ref. (*5*) gives the same rovibrational assignment, [414] (0 1 5), for the three interacting levels. Additional calculations in the frame of the EH method were needed to identify the possible resonance partners of the (0 1 5) bright state. According to Ref. (*5*), two highly excited bending states (0 6 3) at

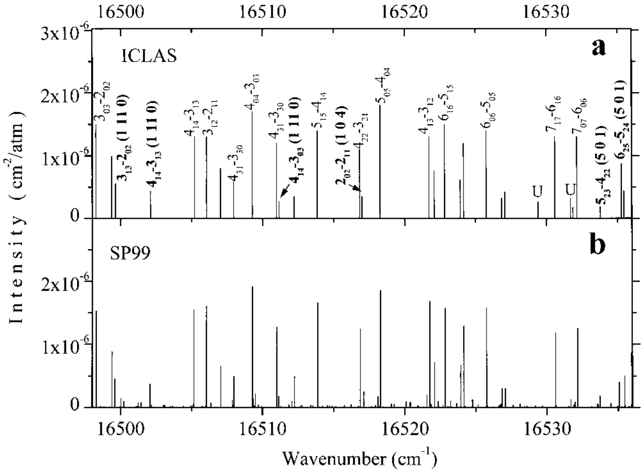

FIG. 2. Comparison of the HDO stick absorption spectrum in the 16 498–16 536 cm^{-1} spectral region. (a) Stick spectrum extracted from the ICLAS spectrum. (b) Calculated spectrum provided by Ref. (*5*). In this region, most of the transitions belong to the $2\nu_2 + 4\nu_3$ band except six lines, labeled in bold character, for which the vibrational assignment is indicated. Two unassigned lines are marked by "U."

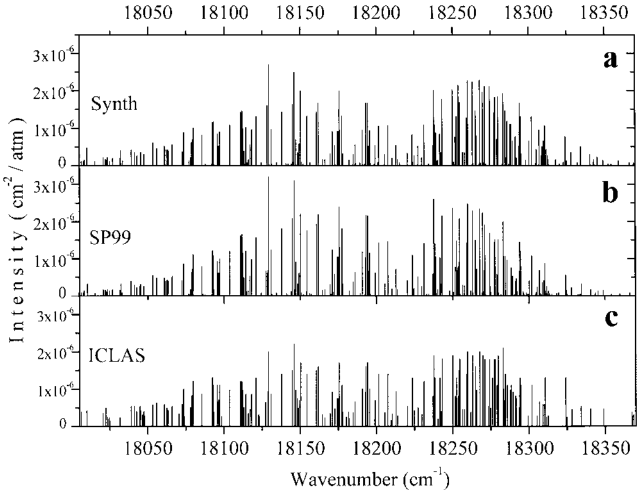

FIG. 3. Comparison of the overview of the $\nu_2 + 5\nu_3$ band of HDO absorption spectrum. (a) Synthetic spectrum obtained in the effective Hamiltonian (EH) approach. (b) Calculated spectrum predicted by the *ab initio* calculations of Ref. (*5*). (c) Stick spectrum retrieved from the ICLAS data. The absolute intensities were obtained after normalization of the experimental data against the corresponding absorption intensity predicted (*5*) in the analyzed region (see text).

TABLE 4

Wavenumbers, Intensities, and Rovibrational Assignments of the Transitions of the $\nu_2 + 5\nu_3$ Band of HDO between 18 000 and 18 350 cm^{-1}

Observed Wavenumber (cm^{-1})	Intensity (cm^{-2}/atm) Obs.	Calc.	Ref.(*5*)	Upper $J K_a K_c$	Lower $J K_a K_c$
18006.201	3.8E-07	1.0E-07	8.7E-08	8 4 4	9 4 5
18009.903	4.2E-07	2.3E-07	1.6E-07	10 0 10	11 0 11
18009.903	4.2E-07	2.3E-07	1.6E-07	10 1 10	11 1 11
18022.381	4.8E-07	1.4E-07	1.1E-07	9 2 7	10 2 8
18022.381	4.8E-07	1.5E-07	1.4E-07	7 4 3	8 4 4
18023.411	2.6E-07	2.1E-07	1.7E-07	9 1 8	10 1 9
18024.898	2.3E-07	6.1E-08	6.7E-08	5 5 0	6 5 1
18024.898	2.3E-07	6.1E-08	6.7E-08	5 5 1	6 5 2
18031.592	2.3E-07	1.8E-07	1.5E-07	8 3 5	9 3 6
18031.871	2.3E-07	3.8E-07	3.2E-07	9 1 9	10 1 10
18031.980	2.3E-07	3.8E-07	3.2E-07	9 0 9	10 0 10
18038.955	5.3E-07	2.0E-07	2.0E-07	6 4 2	7 4 3
18038.955	5.3E-07	2.0E-07	2.0E-07	6 4 3	7 4 4
18041.209	5.3E-07	3.3E-07	2.9E-07	8 2 7	9 2 8
18042.613	3.9E-07	2.5E-07	2.2E-07	8 2 6	9 2 7
18044.945	5.3E-07	2.9E-07	2.8E-07	7 3 5	8 3 6
18045.158	4.3E-07	3.4E-07	3.1E-07	8 1 7	9 1 8
18046.534	3.1E-07				
18047.428	3.9E-07	2.8E-07	2.6E-07	7 3 4	8 3 5
18047.710	2.9E-07				
18053.027	5.3E-07	5.8E-07	5.4E-07	8 1 8	9 1 9
18053.239	5.7E-07	5.8E-07	5.4E-07	8 0 8	9 0 9
18055.741	6.1E-07	2.2E-07	2.4E-07	5 4 1	6 4 2
18055.741	6.1E-07	2.2E-07	2.4E-07	5 4 2	6 4 3
18060.753	5.7E-07	4.9E-07	4.8E-07	7 2 6	8 2 7
18061.153	4.9E-07	4.1E-07	3.9E-07	7 2 5	8 2 6
18062.524	4.8E-07	4.0E-07	4.2E-07	6 3 4	7 3 5
18063.206	4.3E-07	4.0E-07	4.1E-07	6 3 3	7 3 4
18065.914	5.3E-07	5.3E-07	5.2E-07	7 1 6	8 1 7
18070.432	3.3E-07				
18072.443	5.8E-07	1.7E-07	2.0E-07	4 4 1	5 4 2
18072.443	5.8E-07	1.7E-07	2.0E-07	4 4 0	5 4 1
18073.226	9.8E-07	8.3E-07	8.4E-07	7 1 7	8 1 8
18073.612	9.8E-07	8.3E-07	8.5E-07	7 0 7	8 0 8
18078.024	4.9E-07	1.0E-07	8.5E-08	7 6 2	7 6 1
18078.024	4.9E-07	1.0E-07	8.5E-08	7 6 1	7 6 2
18078.628	8.0E-07	6.0E-07	6.3E-07	6 2 4	7 2 5
18079.016	6.4E-07	1.8E-07	1.7E-07	6 6 1	6 6 0
18079.016	6.4E-07	1.8E-07	1.7E-07	6 6 0	6 6 1
18079.366	9.8E-07	6.8E-07	7.3E-07	6 2 5	7 2 6
18079.649	1.2E-06	4.9E-07	5.5E-07	5 3 2	6 3 3
18079.649	1.2E-06	4.9E-07	5.5E-07	5 3 3	6 3 4
18085.423	8.5E-07	7.7E-07	7.8E-07	6 1 5	7 1 6
18092.493	1.3E-06	1.1E-06	1.2E-06	6 1 6	7 1 7
18093.022	1.1E-06	1.1E-06	1.1E-06	6 0 6	7 0 7
*18093.439	3.7E-07		1.5E-07	6 5 2	7 0 7
18095.515	1.1E-06	8.0E-07	9.1E-07	5 2 3	6 2 4
18096.291	6.4E-07	5.1E-07	6.1E-07	4 3 1	5 3 2
18096.479	6.9E-07	5.0E-07	6.1E-07	4 3 2	5 3 3
18097.131	1.1E-06	8.6E-07	1.0E-06	5 2 4	6 2 5
18098.413	2.6E-07				
18103.647	9.5E-07	1.0E-06	1.2E-06	5 1 4	6 1 5
18110.755	1.2E-06	1.4E-06	1.6E-06	5 1 5	6 1 6
18111.321	1.9E-07	6.1E-08	5.1E-08	6 0 6	6 2 5
18111.659	1.2E-06	1.4E-06	1.7E-06	5 0 5	6 0 6
18112.272	9.5E-07	9.4E-07	1.2E-06	4 2 2	5 2 3
18112.979	5.0E-07	3.8E-07	4.8E-07	3 3 0	4 3 1
18113.089	4.9E-07	3.7E-07	4.8E-07	3 3 1	4 3 2
18114.235	8.5E-07	9.7E-07	1.2E-06	4 2 3	5 2 4
18115.927	3.3E-07	1.5E-07	1.3E-07	7 5 3	7 5 2
18116.042	3.3E-07	1.5E-07	1.3E-07	7 5 2	7 5 3
18117.072	4.5E-07	2.7E-07	2.6E-07	6 5 2	6 5 1
18117.072	4.5E-07	2.7E-07	2.6E-07	6 5 1	6 5 2
18118.099	8.5E-07	4.6E-07	4.9E-07	5 5 0	5 5 1
18118.099	8.5E-07	4.6E-07	4.9E-07	5 5 1	5 5 0
18120.931	1.3E-06	1.3E-06	1.6E-06	4 1 3	5 1 4
18123.310	2.6E-07				
**18127.310	6.5E-07		6.6E-07	4 0 4	5 1 5
18128.624	9.1E-07	1.5E-06	6.8E-07	4 1 4	5 1 5
***18128.624	9.1E-07		6.1E-07	4 1 4	5 1 5
18129.167	2.0E-06	9.3E-07	1.2E-06	3 2 1	4 2 2
18129.167	2.0E-06	1.6E-06	1.9E-06	4 0 4	5 0 5
18130.841	8.5E-07	9.4E-07	1.2E-06	3 2 2	4 2 3
18137.753	1.4E-06	1.4E-06	1.8E-06	3 1 2	4 1 3
18144.862	1.5E-06	1.6E-06	2.1E-06	3 1 3	4 1 4
18146.073	2.2E-06	1.7E-06	2.2E-06	3 0 3	4 0 4
18146.073	2.2E-06	6.7E-07	9.1E-07	2 2 0	3 2 1
18146.930	4.8E-07	1.8E-07	1.6E-07	7 4 4	7 4 3
18147.096	9.5E-07	6.6E-07	9.1E-07	2 2 1	3 2 2
18148.260	7.4E-07	3.3E-07	3.3E-07	6 4 3	6 4 2
18148.713	4.7E-07	3.3E-07	3.2E-07	6 4 2	6 4 3
18149.365	6.9E-07	5.7E-07	6.1E-07	5 4 2	5 4 1
18149.454	5.8E-07	5.7E-07	6.1E-07	5 4 1	5 4 2
18150.339	1.7E-06	9.4E-07	1.1E-06	4 4 0	4 4 1
18150.339	1.7E-06	9.4E-07	1.1E-06	4 4 1	4 4 0
18154.421	1.4E-06	1.3E-06	1.8E-06	2 1 1	3 1 2
18160.690	1.5E-06	1.4E-06	1.9E-06	2 1 2	3 1 3
18161.897	1.6E-06	1.6E-06	2.2E-06	2 0 2	3 0 3
18164.592	3.1E-07	1.6E-07	1.4E-07	7 3 5	7 3 4
18166.229	2.3E-07	1.6E-07	1.6E-07	6 2 5	6 2 4
18169.758	3.4E-07	2.9E-07	3.0E-07	6 3 4	6 3 3
18171.149	9.1E-07	8.8E-07	1.2E-06	1 1 0	2 1 1
18172.766	4.7E-07	5.2E-07	5.7E-07	5 3 3	5 3 2
18174.460	7.4E-07	8.8E-07	1.0E-06	4 3 2	4 3 1
18175.212	7.4E-07	8.8E-07	1.0E-06	4 3 1	4 3 2
18175.527	1.5E-06	1.5E-06	1.9E-06	3 3 1	3 3 0
18175.621	1.7E-06	5.1E-07	5.6E-07	5 3 2	5 3 3
18175.621	1.7E-06	1.5E-06	1.9E-06	3 3 0	3 3 1
18175.935	8.0E-07	9.2E-07	1.3E-06	1 1 1	2 1 2
18177.424	1.1E-06	1.3E-06	1.8E-06	1 0 1	2 0 2
18177.667	2.3E-07	2.8E-07	2.8E-07	6 3 3	6 3 4
18177.997	3.7E-07	3.0E-07	3.3E-07	5 2 4	5 2 3
18182.287	2.0E-07	1.4E-07	1.3E-07	7 3 4	7 3 5
18184.770	3.6E-07	2.9E-07	3.7E-07	3 1 3	3 1 2
18186.003	6.4E-07	5.3E-07	6.4E-07	4 2 3	4 2 2
18190.797	9.8E-07	9.2E-07	1.2E-06	3 2 2	3 2 1
18192.926	9.1E-07	7.3E-07	1.0E-06	0 0 0	1 0 1
18193.190	1.6E-06	1.6E-06	2.2E-06	2 2 1	2 2 0
18194.186	1.7E-06	1.6E-06	2.2E-06	2 2 0	2 2 1
18195.582	9.8E-07	9.0E-07	1.2E-06	3 2 1	3 2 2
18198.956	2.0E-07	4.2E-08	3.1E-08	8 1 7	7 3 4
18199.209	6.9E-07	5.1E-07	6.2E-07	4 2 2	4 2 3
18201.573	1.4E-06	1.0E-06	1.4E-06	1 1 1	1 1 0
18205.447	3.6E-07	2.9E-07	3.2E-07	5 2 3	5 2 4
18207.537	1.4E-06	1.0E-06	1.5E-06	1 1 0	1 1 1
18210.285	3.2E-07	9.7E-08	8.9E-08	6 5 2	5 5 1
18210.285	3.2E-07	9.7E-08	8.7E-08	6 5 1	5 5 0
18212.772	9.1E-07	5.2E-07	7.1E-07	2 1 1	2 1 2
18213.864	2.8E-07	1.6E-07	1.7E-07	6 2 4	6 2 5
18220.340	5.3E-07	3.2E-07	4.2E-07	3 1 2	3 1 3
18223.588	1.3E-06	7.9E-07	1.1E-06	1 0 1	0 0 0
18224.736	4.1E-07	1.3E-07	1.0E-07	7 5 3	6 5 2
18224.736	4.1E-07	1.3E-07	1.0E-07	7 5 2	6 5 1
18227.337	4.9E-07	2.5E-07	2.6E-07	5 4 2	4 4 1
18227.337	4.9E-07	2.5E-07	2.6E-07	5 4 1	4 4 0
18229.779	3.1E-07	2.0E-07	2.6E-07	4 1 3	4 1 4
18231.272	1.2E-06	1.1E-06	1.4E-06	2 1 2	1 1 1
18237.113	8.0E-07	5.1E-07	5.8E-07	4 3 2	3 3 1
18237.720	1.9E-06	5.1E-07	5.8E-07	4 3 1	3 3 0
18237.720	1.9E-06	1.5E-06	2.0E-06	2 0 2	1 0 1

Note. The experimental, calculated (EH), and predicted (*5*) intensities are given in cm^{-2}/atm at 296 K and correspond to pure HDO. The total calculated and experimental line intensities were normalized to the total HDO intensity predicted in Ref. (*5*) (see text). T means tentative assignment. The asterisks (*), (**), and (***) mark extra lines of the $\nu_1 + \nu_2 + 4\nu_3$, $6\nu_2 + 3\nu_3$, and $2\nu_1 + 7\nu_2 + \nu_3$ bands, respectively (see text). In the case of unresolved multiplets, the same experimental intensity is given for the different components, while the intensities calculated from the EH or from Ref. (*5*) correspond to each component.

TABLE 4—*Continued*

Observed Wavenumber (cm^{-1})	Intensity (cm^{-2}/atm)			Upper $J\ K_a\ K_c$	Lower $J\ K_a\ K_c$
	Obs.	Calc.	Ref.(*5*)		
18238.394	1.3E-06	1.0E-06	1.4E-06	2 1 1	1 1 0
18240.291	2.0E-07	1.4E-07	1.6E-07	5 1 4	5 1 5
18241.711	1.3E-06	8.2E-07	1.0E-06	3 2 1	2 2 0
18242.330	4.0E-07	3.4E-07	3.2E-07	6 4 2	5 4 1
18243.121	1.8E-06	1.7E-06	2.1E-06	3 1 3	2 1 2
18250.064	1.9E-06	2.0E-06	2.4E-06	3 0 3	2 0 2
18251.678	8.0E-07	7.4E-07	7.7E-07	5 3 3	4 3 2
18252.476	1.3E-06	1.3E-06	1.5E-06	4 2 3	3 2 2
**18252.776	7.5E-07		6.8E-07	4 0 4	3 1 3
18253.595	8.0E-07	7.2E-07	7.6E-07	5 3 2	4 3 1
***18254.087	1.5E-06		7.9E-07	4 1 4	3 1 3
18254.087	1.5E-06	2.1E-06	9.1E-07	4 1 4	3 1 3
18254.545	1.8E-06	1.6E-06	2.1E-06	3 1 2	2 1 1
18254.794	1.4E-07				
18256.627	4.4E-07	3.3E-07	2.8E-07	7 4 4	6 4 3
18257.789	4.5E-07	3.3E-07	2.8E-07	7 4 3	6 4 2
18259.192	1.4E-06	1.2E-06	1.4E-06	4 2 2	3 2 1
18259.784	2.0E-06	2.2E-06	2.5E-06	4 0 4	3 0 3
**18261.832	3.8E-07		1.4E-07	4 0 4	3 0 3
18262.982	1.9E-06	2.2E-06	2.3E-06	5 1 5	4 1 4
18264.967	1.5E-06	1.4E-06	1.5E-06	5 2 4	4 2 3
18265.765	9.5E-07	7.7E-07	7.3E-07	6 3 4	5 3 3
18267.810	2.0E-06	2.2E-06	2.3E-06	5 0 5	4 0 4
18269.709	1.9E-06	1.9E-06	2.2E-06	4 1 3	3 1 2
18270.766	8.5E-07	7.4E-07	6.9E-07	6 3 3	5 3 2
18271.067	1.8E-06	2.0E-06	1.9E-06	6 1 6	5 1 5
18273.354	5.4E-07				
18274.243	1.8E-06	2.0E-06	1.7E-06	6 0 6	5 0 5
*18274.643	4.9E-07		2.6E-07	6 5 2	5 0 5
18274.984	4.9E-07		1.2E-07	6 1 6	5 0 5
18276.153	1.3E-06	1.3E-06	1.3E-06	6 2 5	5 2 4
18277.228	1.8E-06	1.3E-06	1.4E-06	5 2 3	4 2 2
18277.810	1.8E-06	1.8E-06	1.5E-06	7 1 7	6 1 6
18279.042	1.1E-06	6.8E-07	5.7E-07	7 3 5	6 3 4
18279.801	1.9E-06	1.8E-06	1.5E-06	7 0 7	6 0 6
18283.172	2.1E-06	1.9E-06	2.0E-06	5 1 4	4 1 3
18283.349	9.8E-07	1.4E-06	1.1E-06	8 1 8	7 1 7
18284.506	1.4E-06	1.4E-06	1.1E-06	8 0 8	7 0 7
18285.828	1.1E-06	1.1E-06	9.7E-07	7 2 6	6 2 5
18287.776	9.5E-07	1.1E-06	7.6E-07	9 1 9	8 1 8
18288.383	1.1E-06	1.0E-06	7.5E-07	9 0 9	8 0 8
18289.529	9.1E-07	6.4E-07	5.3E-07	7 3 4	6 3 3
18291.127	6.9E-07	7.3E-07	4.6E-07	10 1 10	9 1 9
18291.239	8.0E-07	5.3E-07	3.9E-07	8 3 6	7 3 5
18291.488	7.4E-07	7.3E-07	4.6E-07	10 0 10	9 0 9
18293.711	5.0E-07	4.8E-07	2.5E-07	11 0 11	10 0 10
18293.878	8.5E-07	8.7E-07	6.6E-07	8 2 7	7 2 6
18294.088	1.3E-06	1.6E-06	1.5E-06	6 1 5	5 1 4
18294.742	1.1E-06	1.2E-06	1.2E-06	6 2 4	5 2 3
18301.943	1.1E-06	1.2E-06	1.1E-06	7 1 6	6 1 5
T18305.227	2.7E-07	4.1E-07	2.4E-07	10 2 9	9 2 8
18306.978	6.4E-07	9.1E-07	6.9E-07	8 1 7	7 1 6
18309.009	5.8E-07	4.8E-07	3.6E-07	8 3 5	7 3 4
18309.898	5.8E-07	6.2E-07	4.2E-07	9 1 8	8 1 7
18310.692	1.0E-06	1.0E-06	8.7E-07	7 2 5	6 2 4
18311.620	2.5E-07	4.1E-07	2.4E-07	10 1 9	9 1 8
18312.644	2.8E-07	2.5E-07	1.3E-07	11 1 10	10 1 9
18324.147	6.0E-07	7.3E-07	5.6E-07	8 2 6	7 2 5
18324.931	2.4E-07	1.2E-07	1.5E-07	4 2 2	3 0 3
T18328.119	4.4E-07	3.3E-07	2.2E-07	9 3 6	8 3 5
18334.210	5.3E-07	4.7E-07	3.1E-07	9 2 7	8 2 6
18340.380	4.5E-07	2.8E-07	1.6E-07	10 2 8	9 2 7
18348.902	4.5E-07	1.3E-07	1.5E-07	5 2 3	4 0 4

18 202 cm^{-1} and (2 7 1) at 18 163 cm^{-1} could perturb the $K_a = 0, 1$ energy levels of the (0 1 5) state. This resonance is a consequence of the relative values of the vibrational energy and rotational constants of the three interacting states. After considering the predicted energy levels of the (0 6 3) and (1 7 2) states (*5*), we conclude that the rovibrational states perturbing the [4 1 4] (0 1 5) level should, in fact, be labeled as [404] (0 6 3) and [414] (2 7 1) states. Indeed, we found three extra lines reaching the [404] (0 6 3) level in the recorded spectrum (see Table 5 and Fig. 4). However, two more extra lines reaching the [414] (2 7 1) level and predicted (*5*) with significant intensity were not observed in the ICLAS spectrum. These lines correspond to the 4_{14}–3_{13} (7.9×10^{-7} cm^{-2}/atm) and 4_{14}–5_{15} (6.1×10^{-7} cm^{-2}/atm) transitions of the (2 7 1) state predicted (*5*) at 18 254.48 and 18 129.00 cm^{-1}, respectively. As we achieved very good agreement between the predicted (*5*) and measured line intensities throughout the spectrum, we examine this situation in more detail and conclude that the above predicted lines are in fact blended with the similar transitions of the $\nu_2 + 5\nu_3$ band at 18 254.087 and 18 128.624 cm^{-1} (see Fig. 4). In other words, the [414] energy level of the (2 7 1) state is found in coincidence, within the experimental uncertainty limit, with that of the (0 1 5) state. This accidental degeneracy may give an interesting opportunity for studying line mixing effects through a detailed investigation of the pressure dependence of this line profile. Figure 4 shows the comparison between the ICLAS spectrum, the *ab initio* predictions (*5*), and the EH synthetic spectrum in the 18 247–18 275 cm^{-1} spectral region, including the 4_{14}–3_{13} transition of the $\nu_2 + 5\nu_3$ band. According to Ref. (*5*), this last line is predicted to be split into three transitions marked by the upper arrows, while the lower arrows indicate the two experimental absorption lines corresponding to the above three predicted transitions.

The occurrence of other less pronounced resonance perturbations is revealed by significant deviations obtained for some of the $K_a = 0, 1$ energy levels included into the fitting. In particular, the fitted vibrational term value (18 208.380 cm^{-1}) deviates by 0.054 cm^{-1} from the energy value of the [000] level. On the basis of the predictions of Ref. (*5*), it appears that the slight perturbation affecting the (0 1 5) [606] sublevel is due to an accidental resonance with the (1 1 4) [652] sublevel. The identification of this resonance which takes place for levels with a large difference of K_a values could not have been expected from the mere comparison of the vibrational term value of the (0 1 5) and (1 1 4) states, separated by more than 350 cm^{-1}. It has only been possible on the basis of the predictions of Ref. (*5*). Though the resonance shift of the (1 0 5) [6 0 6] energy level is rather limited, the intensity transfer is

TABLE 5

Rotational Energy Levels (cm^{-1}) of the (0 1 5) Vibrational State of HDO

$J\,K_a\,K_c$	E_{obs}	σ	N	obs.-calc	Δ
0 0 0	18208.434		1	0.054	0.73
1 0 1	18223.592	0.005	2	0.069	0.71
1 1 1	18234.065	0.004	2	-0.027	0.72
1 1 0	18237.339	0.006	2	-0.032	0.72
2 0 2	18253.227	0.001	2	0.076	0.71
2 1 2	18261.080	0.001	2	-0.017	0.79
2 1 1	18270.890	0.007	3	-0.033	0.71
2 2 1	18302.472	0.013	2	-0.015	0.69
2 2 0	18303.124	0.013	2	-0.011	0.69
3 0 3	* 18296.233	0.004	2	0.131	0.69
3 1 3	18301.241	0.007	3	0.020	0.71
3 1 2	18320.732	0.003	3	-0.028	0.71
3 2 2	18347.872	0.011	2	-0.015	0.69
3 2 1	18350.975	0.005	2	0.007	0.69
3 3 1	18408.577	0.001	2	0.012	0.65
3 3 0	18408.650	0.006	2	0.003	0.65
4 0 4	* 18351.113	0.001	2	-0.126	0.75
4 1 4	* 18354.483	0.006	2	0.376	1.00
4 1 3	18386.166	0.004	3	-0.022	0.71
4 2 3	18407.868	0.003	2	-0.004	0.70
4 2 2	18416.258	0.006	4	-0.002	0.69
4 3 2	18470.139	0.004	3	0.005	0.65
4 3 1	18470.700	0.001	2	0.008	0.65
4 4 1	18552.677	0.008	2	0.021	0.59
4 4 0	18552.685	0.017	2	0.020	0.59
5 0 5	18417.970	0.004	2	-0.009	0.71
5 1 5	18419.367	0.003	2	-0.059	0.71
5 1 4	18466.155	0.001	3	0.001	0.68
5 2 4	18482.002	0.008	3	0.001	0.67
5 2 3	18499.062	0.003	3	0.001	0.67
5 3 3	18547.168	0.005	3	0.006	0.64
5 3 2	18549.279	0.007	2	0.012	0.64
5 4 2	18629.627	0.004	2	0.007	0.59
5 4 1	18629.704	0.007	2	0.009	0.59
5 5 1	18734.066	0.002	2	-0.007	0.53
5 5 0	18734.066	0.001	2	-0.007	0.53
6 0 6	18496.189	0.005	3	-0.046	0.81
6 1 6	18496.935	0.003	2	0.016	0.68
6 1 5	18559.332	0.008	2	0.006	0.66
6 2 5	18569.787	0.007	3	0.011	0.66
6 2 4	18598.742	0.006	3	0.011	0.67
6 3 4	18639.427	0.004	3	-0.010	0.65
6 3 3	18645.175	0.006	3	-0.009	0.63
6 4 3	18722.230		1	-0.008	0.59
6 4 2	18722.596	0.007	2	-0.001	0.60
6 5 2	18826.246	0.007	2	-0.001	0.52
6 5 1	18826.246	0.008	2	-0.009	0.52
6 6 1	18951.806		1	-0.011	0.41
6 6 0	18951.806		1	-0.011	0.43
7 0 7	18586.121	0.006	2	0.023	0.71
7 1 7	18586.429	0.004	2	0.022	0.71
7 1 6	18664.463	0.014	2	-0.006	0.68
7 2 6	18670.701	0.002	2	0.009	0.65
7 2 5	18714.242	0.001	2	0.014	0.69
7 3 5	18746.558	0.005	3	-0.038	0.65
7 3 4	* 18759.192	0.001	2	0.141	0.62
7 4 4	18830.528	0.011	2	-0.003	0.59
7 4 3	18831.766	0.007	2	-0.006	0.66
7 5 3	* 18933.921	0.019	2	-0.090	0.54
7 5 2	18934.048		1	-0.012	0.43
7 6 2	19059.152		1	0.016	0.41
7 6 1	19059.152		1	0.015	0.46
8 0 8	18687.667	0.001	2	0.020	0.80
8 1 8	18687.806	0.012	2	0.024	0.80
8 1 7	18780.894	0.001	2	-0.001	0.67
8 2 7	18784.305	0.001	2	0.007	0.66
8 2 6	18844.263	0.007	2	0.027	0.74
8 3 6	18868.143		1	-0.010	0.61
8 3 5	* 18890.977	0.007	2	0.166	0.63
8 4 4	18957.836		1	0.019	0.67
9 0 9	18800.904	0.006	2	-0.014	1.07
9 1 9	18800.985	0.002	2	0.008	1.07
9 1 8	18908.468	0.007	2	-0.010	0.72
9 2 7	18987.298		1	0.010	0.99
10 0 10	18925.924	0.008	2	0.002	1.14
10 1 10	18925.918		1	-0.029	1.26
10 1 9	19047.355		1	0.001	0.95
10 2 8	19142.024		1	-0.043	1.05
11 0 11	19062.641		1	-0.006	1.76
11 1 10	19197.708		1	0.030	1.05
		(114)			
6 5 2	18496.595	0.005	2		-0.06
		(063)			
4 0 4	18353.168	0.005	3		0.82
		(271)			
4 1 4	18354.483	0.006	2		0.39

Note. Asterisks denote the energy levels excluded from the fitting. σ denotes the experimental uncertainty of the level in cm^{-1}. N is the number of lines sharing the same upper level. Δ is the difference between the experimental energy levels and the predictions of Ref. (*5*).

sufficient to give rise to two weak extra lines reaching the (1 1 4) [652] upper level (see Table 4).

CONCLUSION

The weak absorption bands of HDO surrounding the stronger $5\nu_3$ band at 16 920.02 cm^{-1} have been studied in the frame of the effective Hamiltonian model. Interestingly, the (0 1 5) vibrational state, which is the most excited state of HDO analyzed so far, is found mostly decoupled from the nearby vibrational states. The (0 2 4) state at 16 456 cm^{-1} is coupled to a number of vibrational states, some of which could be identified only by considering the results of the *ab initio* calculations of Schwenke and Partridge (*5*). The effective Hamiltonian approach applied to this interacting system has allowed us to retrieve the effective rovibrational parameters of the (0 2 4), (1 0 4), and (5 0 1) interacting states.

Our systematic ICLAS investigation of the HDO overtone spectrum between 13 000 and 18 500 cm^{-1} has proven the high quality of the results obtained by Schwenke and Partridge both

TABLE 6
Spectroscopic Constants of the (0 1 5) Vibrational State of HDO (in cm^{-1})

E_v	18208.3801(900)
A	19.79283(300)
B	9.217575(700)
C	5.928537(400)
Δ_K	1.3194(200) × 10^{-2}
Δ_{JK}	-6.964(200) × 10^{-4}
Δ_J	5.0842(200) × 10^{-4}
δ_k	2.2515(200) × 10^{-3}
δ_j	2.0332(200) × 10^{-4}
H_k	4.333(600) × 10^{-5}

for line positions and intensities. In particular, the deviations between the observed and predicted energy levels do not show any significant trends over the whole spectral range. In contrast, the highly excited regions considered in the present paper are among the best predicted ones with an average deviation as low as -0.06 cm^{-1} in the 16 300–16 670 cm^{-1} region.

As a general comment concerning the anharmonic couplings in HDO, it appears that, in addition to the regular Fermi-type resonance, high-order anharmonic interactions between the (V_1, V_2, V_3) vibrational state and ($V_1 \pm 2$, $V_2 \mp 4$, V_3), ($V_1 \pm 3$, $V_2 \mp 6$, V_3), ($V_1 \pm 1$, $V_2 \pm 3$, $V_3 \mp 2$), (V_1, $V_2 \pm 5$, $V_3 \mp 2$), ($V_1 \pm 1$, $V_2 \mp 8$, $V_3 \pm 2$) states together with minor rovibrational couplings can affect the HDO rovibrational energy levels destroying possible polyad structure. Accounting for these interactions in the frame of the effective Hamiltonian method is hindered by the necessity of a correct estimation of rotational and centrifugal distortion constants of the high-bending states. However, the rovibrational energy levels and line intensities could be modeled, in most cases, in the frame of the EH model. This well-established approach, which has the advantage of being compact, has allowed us to fix some ambiguous rovibrational assignments provided in Ref. (*5*), to test and confirm *ab initio* intensity calculations, and, in certain cases, to provide more accurate line position predictions compared to Ref. (*5*). Finally, the joint application of these two theoretical approaches to the spectra analysis has added to the reliability of the HDO spectra assignment and prediction.

ACKNOWLEDGMENTS

O. Naumenko thanks the University Joseph Fourier of Grenoble for the Visiting Professorship, during which this work was carried out, and acknowledges as well

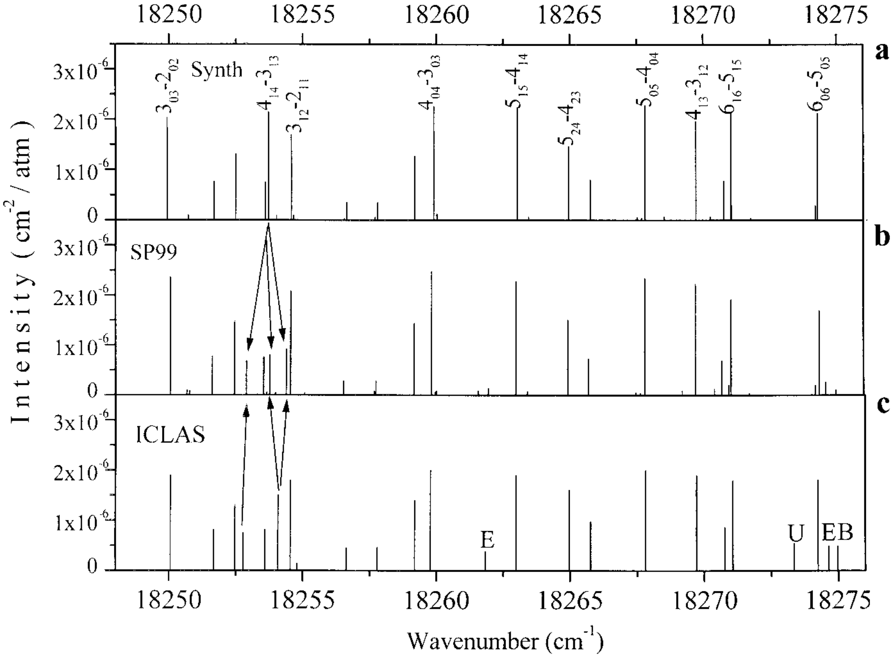

FIG. 4. Comparison of the HDO stick absorption spectrum in the 18 247–18 275 cm^{-1} spectral region. (a) Stick spectrum extracted from the ICLAS spectrum. (b) Calculated spectrum provided by the *ab initio* calculations of Ref. (*5*). For easier comparison with the experimental data, all the predicted frequencies were decreased by 0.7 cm^{-1}. (c) Synthetic spectrum obtained from the effective Hamiltonian (EH) approach. The upper arrows mark the 4_{14}–3_{13} unperturbed transition of the $\nu_2 + 5\nu_3$ band which is predicted (*5*) split into three components due to resonance interaction with levels of the (0 6 3) and (2 7 1) vibrational states. The lower arrows indicate the two observed lines corresponding to the above three predicted transitions (see text). Two more identified extra lines (E) are observed in agreement with Ref. (*5*). The only observed transition of *b* type is also marked (B). One unassigned line (may be due to H_2O) is marked by "U."

the financial support from the Russian Foundation for Basic Researches, Grant 99-03-33210. The expert help of G. Weirauch during the recording of the spectra is also acknowledged. We are grateful to D. Schwenke and H. Partridge for access to the results of their HDO calculations before publication.

REFERENCES

1. O. Naumenko, E. Bertseva, and A. Campargue, *J. Mol. Spectrosc.* **197,** 122–132 (1999).
2. O. Naumenko and A. Campargue, *J. Mol. Spectrosc.* **199,** 59–72 (2000).
3. O. Naumenko, E. Bertseva, A. Campargue, and D. Schwenke, *J. Mol. Spectrosc.* **201,** 297–309 (2000).
4. E. Bertseva, O. Naumenko, and A. Campargue, **203,** 28–36 (2000).
5. D. Schwenke and H. Partridge, *J. Chem. Phys.*, in press.
6. A. Perrin, J.-M. Flaud, and C. Camy-Peyret, *J. Mol. Spectrosc.* **112,** 156–162 (1985).
7. A. Perrin, J.-M. Flaud, and C. Camy-Peyret, *Can. J. Phys.* **64,** 736–742 (1986).
8. T. Ohshima and H. Sasada, *J. Mol. Spectrosc.* **136,** 250–263 (1989).
9. A. D. Bykov, O. V. Naumenko, L. N. Sinitsa, B. P. Winnewisser, M. Winnewisser, P. S. Ormsby, and K. Narahari Rao, *SPIE* **2205,** 248–252 (1993).
10. A. D. Bykov, O. V. Naumenko, T. M. Petrova, L. N. Sinitsa, and B. A. Voronin, *Atmos. Oceanic. Opt.* **19,** 1281–1289 (1999).
11. A. D. Bykov, O. V. Naumenko, and L. N. Sinitsa, *Atmos. Opt.* **3,** 1015–1025 (1990).
12. M. Herman, J. Liévin, J. Van der Auwera, and A. Campargue, *Adv. Chem. Phys.* **108,** 1–431 (1999).
13. A. Campargue, M. Chenevier, and F. Stoeckel, *Spectrochim. Acta Rev.* **13,** 69–88 (1990).
14. S. Gerstenkorn and P. Luc, “Atlas du Spectre d’Absorption de la Molécule d’Iode,” Edition du CNRS, Paris, 1978.
15. L. S. Rothman, C. P. Rinsland, A. Goldman, S. T. Massie, D. P. Edwards, J.-M. Flaud, A. Perrin, C. Camy-Peyret, V. Dana, J.-Y. Mandin, J. Schroeder, A. McCann, R. R. Gamache, R. B. Wattson, K. Yoshino, K. V. Chance, K. W. Jucks, L. R. Brown, V. Nemtchinov, and P. Varanasi, *J. Quant. Spectrosc. Radiat. Transfer* **60,** 665–710 (1998).
16. M. Carleer, A. Jenouvrier, A.-C. Vandaele, P. F. Bernath, M. F. Mérienne, R. Colin, N. F. Zobov, O. L. Polyansky, and J. Tennyson, *J. Chem. Phys.* **111,** 2444–2450 (1999).
17. R. Toth, *J. Mol. Spectrosc.* **162,** 20–40 (1993).
18. O. L. Polyansky, *J. Mol. Spectrosc.* **112,** 79–87 (1985).
19. J.-M. Flaud, C. Camy-Peyret, A. Bykov, O. Naumenko, T. Petrova, A. Scherbakov, and L. N. Sinitsa, *J. Mol. Spectrosc.* **183,** 300–309 (1997).